Indian Journal of Biochemistry & Biophysics
Vol. 59, May 2022, pp. 565-574

Hibiscus tiliaceus mediated phytochemical reduction of zinc oxide nanoparticles and demonstration of their antibacterial, anticancer, and dye degradation capabilities

Vinay Viswanath Konduri[1], Naveen Kumar Kalagatur[2], Anusuya Nagaraj[3], Venkateswara Rao Kalagadda[4], Usha Kiranmayi Mangamuri[1], Chandrasai Potla Durthi[5] & Sudhakar Poda[1]*

[1]Department of Biotechnology, Acharya Nagarjuna University, Guntur-522 510, Andhra Pradesh, India

[2]DRDO-BU-Centre for Life Sciences, Coimbatore-641 046, Tamil Nadu, India

[3]Department of Biochemistry, Bharathiar University, Coimbatore-641 046, Tamil Nadu, India

[4]Center for Nanoscience and Technology, Jawaharlal Nehru Technological University, Hyderabad-500 085, Telangana, India

[5]Department of Biotechnology, National Institute of Technology, Warangal-506 004, Telangana, India

Received 29 December 2021; *revised 11 May 2022*

The present research focused on the green, non-toxic, low-cost synthesis of zinc oxide nanoparticles (ZnO NPs) using aqueous extract of *Hibiscus tiliaceus* leaves as a reducing and stabilizing agent. Thus, synthesized ZnO NPs were characterized by nanotechnological applications, *i.e.*, ultraviolet-visible spectroscopy (UV-vis), dynamic light scattering (DLS), zeta potential, X-ray diffraction (XRD), Fourier transform infrared spectroscopy (FTIR), and high-resolution transmission electron microscopy (HR-TEM). The nanotechnological applications showed that as-synthesized ZnO NPs have bandgap energy of 2.97 eV, zeta potential of −1.2 mV, crystalline in nature (JCPDS data card no-89-1397), and an average size of 30 to 60 nm. The FTIR showed that ZnO NPs have coated with plant secondary metabolites and assisted in the process of green synthesis. The ZnO NPs exhibited broad-spectrum antibacterial activity on Gram-positive and Gram-negative bacteria. The ZnO NPs showed potential anticancer activity against human breast cancer cells MCF-7 and determined the IC_{50} value as 65.83 ± 2.57 µg/mL by MTT assay. Furthermore, ZnO NPs were used as nano-catalyst for dye degradation of methylene blue, methyl orange, and malachite green with $NABH_4$ as a reducing agent. The ZnO NPs exhibited potent dye degradation capability and followed pseudo-first order kinetics. The study concluded that ZnO NPs could be highly useful as anticancer and antibacterial agents in the biomedical field, and as an environmental cleaning agent for dye degradation in textile industries.

Keywords: Antibacterial, Anticancer, *Hibiscus tiliaceus*, Nano-catalyst, Pseudo-first-order kinetics, Zinc oxide nanoparticles

The advent of multidrug-resistant organisms is a substantial worldwide health problem that necessitates the research and development of new therapeutic interventions. Due to the rapid emergence of new resistance mechanisms and a decrease in the efficacy of treating common infectious diseases, microbial responses to routine therapy fail, resulting in extended sickness, increased healthcare costs, and a high risk of mortality. Almost all potential infectious pathogens (*e.g.*, bacteria, fungi, virus, and parasite) have used high degrees of multidrug resistance (MDR), which has resulted in increased morbidity and mortality; consequently, they are known as "superbugs". Although MDR is a natural phenomenon, improper antimicrobial drug use, insufficient hygienic conditions, improper food handling, and poor infection prevention and control procedures all contribute to the establishment of MDR and increase its spread[1]. In the same way, cancer appears in a variety of forms, all of which are characterized by unregulated cell proliferation. There are a variety of methods available to manage this main cause of death. Surgery, radiation therapy, and chemotherapy have demonstrated remarkable efficacy in the treatment of cancer, but they are not without limitations[2].

Also, organic effluents are harmful in nature and constitute a significant threat to life forms that come into contact with them. The majority of the leather, textiles, and pharmaceutical industries discharge this waste into bodies of water, making the water more

*Correspondence:
Phone: +91-9000122929 (Mob)
E-mail:sudhakarpodha@gmail.com

harmful. Non-biodegradable dyes are commonly used in industries, and they are released as effluents, causing harm to live things. To promote living forms healthier, these dyes must be degraded in a more simple and environmentally acceptable manner[3].

In these circumstances, nanoparticles antibacterial and dye degrading properties make nanoparticles effective weapons in the fight against drug-resistant human diseases and dye effluents. Nanoparticles have unique properties such as large surface-to-volume ratio, high dispersion, high penetration, high conductivity, and unique adsorption characteristics. Consequently, these characteristics of nanoparticles enable them to be extensively applied in various fields[3].

For the manufacture of nanoparticles, physical and chemical procedures such as solvothermal, hydrothermal, sol-gel[4], micro-emulsion, vapor phase transport process[5], and precipitation[6] are frequently recommended. These traditional methods take much less time to synthesize large amounts of nanoparticles and use harmful compounds as capping agents for stability, resulting in environmental hazards. Green route synthesis of nanoparticles using plants or plant materials is gaining popularity as an environmentally friendly, biocompatible, large-scale production, and cost-effective option in contrast[7,8]. Biomolecules operate like a reducing as well as a natural capping agent. The interaction of bioactive molecules, enzymes, proteins, and/or other reducing agents with electron-shutting chemicals involved in metal nanoparticle synthesis. Zinc oxide is used in transparent electronics, ultraviolet (UV) light emitters, piezoelectric devices, chemical sensors, spin electronics, personal care products, coatings and paints, and catalytic activities because of its semiconducting, piezoelectric, and pyroelectric qualities[9-11]. Because of its lower cost, UV blocking capabilities, catalytic activity, large surface to area ratio, the broad bandgap of 3.3 eV at ambient temperature, and high exciton binding energy of 60 meV, ZnO NPs have an advantage over other metal nanoparticles[12,13]. Plants such as *Syzygium aromaticum*[14], *Phoenix loureiroi*[15], and *Melia azedarach*[16] have been found to produce ZnO NPs.

The current study focused to synthesize zinc oxide nanoparticles (ZnO NPs) from *Hibiscus tiliaceus* leaves aqueous extract and investigating their benefits. As per our knowledge, this is the first study to report the green synthesis of ZnO NPs from *H. tiliaceus* leaves extract. The beneficial applications of ZnO NPs include antibacterial, anticancer, and degradation of methylene blue (MB), methyl orange (MO), and malachite green (MG) dyes.

Materials and Methods

Chemicals and reagents

Zinc acetate dehydrate (99.99%), Folin-Ciocalteu reagent, sodium carbonate, gallic acid, sodium nitrite, aluminium chloride, sodium hydroxide, methylene blue, malachite green, and methyl orange were purchased from Sigma Aldrich, Bengaluru, India. All glassware was purchased from Borosil, Mumbai, India, and was thoroughly cleaned and rinsed with sterile distilled water before being used in the experiments. The plasticware used in the study was from Tarsons products, Kolkata, India. The other chemicals used in the experiments belonged to analytical grade and were obtained from Merck, Bengaluru, India.

Preparation of plant extract

The leaves of *Hibiscus tiliaceus* were collected from the campus of Acharya Nagarjuna University, India. The voucher was identified and safeguarded in the department of biotechnology, Acharya Nagarjuna University, India. The aqueous leaf extract of *H. tiliaceus* was obtained by boiling 6 g of leaf powder in 100 mL of deionized water for 15 min at 80°C. The extract was then filtered using Whatman no.1 filter paper and stored in the refrigerator at 4°C for further research.

Quantification of total phenolic and flavonoid content of plant extract

Quantification of total phenolic content

According to Javanmardi *et al*. the total phenolic content of plant extract was determined using the Folin-Ciocalteu reagent[17]. Briefly, 2.5 mL of diluted Folin-Ciocalteu reagent and 2 mL of 7.5% (w/v) sodium carbonate were added to 50 µL of plant extract (1 mg/mL) and incubated at 45°C for 15 min. At 765 nm, the absorbance was measured. The results were calculated using a gallic acid calibration curve and expressed as mg of gallic acid equivalents (GAE) per g of leaf extract.

Quantification of total flavonoid content

The total flavonoid content of plant extract was measured using a modified Yu *et al*. colorimetric technique[18]. Briefly, 1 mL of extract (1 mg/mL), 1 mL of distilled water, and 75 µL of sodium nitrite were added to 1 mL of extract (1 mg/mL). Next, 75 µL of 10% $AlCl_3$ solution was added after 5 min. After allowing the mixture to settle for another 5 min, 0.5 mL of 1 M sodium hydroxide was introduced. The reaction mixture was stirred and set aside for 15 min.

At 510 nm, the rise in absorbance was measured. Standard quercetin equivalent (QE) per g of plant extract was used to calculate the total flavonoid content.

Biosynthesis of ZnO NPs

The biosynthesis of zinc oxide nanoparticles (ZnO NPs) was undertaken following Singh *et al*[19]. Briefly, under continual stirring conditions, 2 M of zinc acetate dehydrate [Zn $(CH_3COO)_2]2H_2O$ was prepared in 100 mL deionized water. Under magnetic stirring, 5 mL of plant extract was added to a zinc acetate dehydrate solution, and 2 M of NaOH was added to raise the pH to 12, which is optimal for the synthesis of ZnO NPs. A white precipitate formed after the mixture was agitated constantly for 2 h. To eliminate the contaminants, the precipitate was filtered and washed multiple times with distilled water and then ethanol. After overnight dehydration, the product was a white powder. A color shift was used to visually identify nanoparticle synthesis, and UV-DRS spectrum analysis was used to confirm it.

Characterization of ZnO NPs

The synthesis of ZnO NPs was observed using a double beam UV-DRS spectrophotometer with a wavelength range of 300 to 600 nm to measure the reaction sample (UV-vis DRS 3600- SHIMADZU). To verify the involvement of biomolecules in the reduction process and generation of ZnO NPs, an FTIR spectrum was acquired from a Bruker Alpha II instrument with a wavenumber range of 500 – 4,000 cm^{-1}. The DLS particle size analyzer (Horiba SZ 100) was used to determine the size of the ZnO NPs in colloidal form, as well as zeta potential to investigate the ZnO NPs stability. The crystalline structure of the ZnO NPs was investigated using XRD at 2θ range from 10 to 90° (Bruker D8). High-resolution transmission electron microscopy was used to investigate the size and morphology of ZnO NPs (JSM 2100FJ EOL HR-TEM). The same device was used to do elemental analysis.

Antimicrobial activity of ZnO NPs

The antimicrobial property of ZnO NPs was evaluated against two Gram-positive - *Bacillus subtilis* (MTCC - 441), *Staphylococcus aureus* (MTCC - 1430), and four Gram-negative: *Escherichia coli* (MTCC - 443), *Klebsiella pneumoniae* (MTCC - 7162), *Pseudomonas aeruginosa* (MTCC - 4996), and *Proteus vulgaris* (MTCC - 744), which were obtained from MTCC, Chandigarh, India. A well-diffusion agar plate technique was used to study this property. The bacterial strains were sub-cultures in Lysogeny broth (LB) broth at 37C overnight. The colony-forming unit (CFU) was around 2.5×10^{-5} which was adjusted with 0.5 McFarland constant and an OD measured at 600 nm using UV-Vis spectrophotometer[8]. The sub-cultured strains were swabbed onto the Lysogeny agar (LA) plate, for which a cork borer was used to make the wells. A 100 µL of synthesized ZnO NPs were added to wells with different concentrations. Later, the plates were incubated at 37C for overnight observation. The diameter of the inhibition zone was measured with a zone scale in mm.

Anticancer activity of ZnO NPs

Cell culture and maintenance

MCF-7 cells (human breast cancer) cells were obtained from National Center for Cell Sciences (NCCS), Pune, India. The cells were grown in Dulbecco's modified eagle's medium (DMEM) with 10% of fetal bovine serum (FBS), 1% of L-glutamine, and 1% of streptomycin-penicillin in a humidified chamber at 5% CO_2 and 37°C. The cells were grown to attain 80-90% confluence by providing the fresh media alternative days[20].

Treatment of ZnO NPs

Anticancer activity of ZnO NPs was carried out by MTT assay and methodology was adopted from Swaminathan *et al*., with minor modifications[21]. Briefly, 1×10^4 cells were seeded in a 96-well cell culture plate and allowed for overnight to adhere. Following, different concentrations of ZnO NPs were treated to cells in DMEM without FBS and incubated in a humidified chamber at 5% CO_2 and 37°C. Next, 20 µL of MTT (5 mg/mL) was pipetted in and 3 h of incubation was allowed at 25 ± 2°C for 3 h. Following, 100 µL of DMSO was replaced with MTT solution to liquefy the formazan crystals. An absorbance λ_{max} at 570 nm was observed in the microplate reader (Synergy H1, BioTek, USA). The results of the study were expressed with respect to control (100%).

Dye degradation activity of ZnO NPs

Methylene blue (MB), methyl orange (MO), and malachite green (MG) were tested for dye degradation. The dye concentrations were constant throughout the experiment, *i.e*., 1 mM of dye concentration, and $NaBH_4$ was prepared at a concentration of 10 mM, which remained constant throughout the experiment. For

homogeneous mixing, 1 mL of 10 mM sodium borohydride solution was added to 10 mL of 1 mM each dye solution separately and agitated for 5 min. Following, 1 mL of synthesized ZnO NPs (1 mg/mL) was added to each dye solution and mixed individually, and UV-vis spectra absorbance values were obtained at regular intervals.

Statistical analysis

The experiments were performed independently in six replicates (n = 6) and obtained results were stated as mean ± standard deviation. The obtained data were analyzed by one-way ANOVA following Student's *t*-test. The statistical significance was determined at a *P*-value ≤ 0.05.

Results and Discussion

Phytochemical profile of *H. tiliaceus*

Several phytochemicals found in plants, such as polyphenols, flavonoids, terpenoids, and high-low molecular weight proteins, help to produce nanoparticles by reducing their precursor salts and stabilizing the nanoparticles in a complicated redox-mediated process. Therefore, in the present study, quantification of the total phenolics and flavonoids in *H. tiliaceus* leaves extract has been considered to measure their potential to reduce and stabilize the ZnO NPs. The total phenolics and flavonoids of *H. tiliaceus* leave extract were determined by Folin-Ciocalteu and aluminum chloride colorimetric method, respectively (Fig. 1). The study showed that *H. tiliaceus* leaves extract contains a decent amount of total phenolics and flavonoids. The total quantity of phenolics and flavonoids were determined as 16.18 ± 0.98 mg GAE/g and 12.29 ± 0.44 mg QE/g, respectively. The quantity of total phenolics and flavonoids in *H. tiliaceus* leaves extract was found in a dose-dependent manner with the quantity of leaves extract. In support of our study, earlier reports of Wong *et al*. reported total phenolic in leaf as 2080 ± 419 mg GAE/100 g and flower as 2420 ± 167 mg GAE /100 g[22]. Best of our knowledge, previous reports have not existed on the flavonoid content of *H. tiliaceus*. Our study, concludes that *H. tiliaceus* leaves extract was found to be high in phenolics and flavonoids, which could aid in the reduction and stabilization of ZnO NPs.

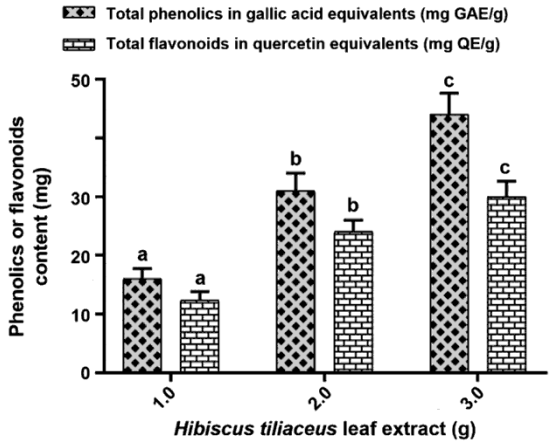

Fig. 1 — Total content of phenolics and flavonoids in *Hibiscus tiliaceus* leaf extract. The experiments were executed in six replicates (n = 6). The results were represented as mean ± standard deviation. The data were analyzed by one-way ANOVA and statistical difference between test samples was analyzed by Tukey's test. The *P*-value ≤ 0.05 was considered significant. The bars in the respective study with different alphabetic was significant (*P*-value ≤ 0.05)

Characterization of ZnO NPs

UV-DRS analysis

Figure 2A shows the optical absorption spectra of ZnO NPs synthesized from *H. tiliaceus* leaf extracts. A prominent and high absorption peak between 300 and 400 nm was seen in the sample, confirming the production of ZnO NPs. Using the following formulae, the bandgap energy (E_g) of Zn O may be calculated from the wavelength value corresponding to the spectrum:

$$E_g = (1240)/\lambda(eV)$$

where, E_g is the bandgap energy (eV) and λ is the wavelength (nm).

In the present study, the corresponding bandgap value was 2.97 eV, indicated that the absorption shift is blue. Generally, the smaller the particle, the larger the band gap patterns should be. The inherent bandgap absorption of ZnO NPs in the wavelength range of 300-400 nm is responsible for the absorption peak. Thus, electrons transition from the valence band to the conduction band[23,24].

FTIR analysis

Figure 2B depicts the FTIR spectrum of as-synthesized ZnO NPs. The ZnO NPs mediated by *H. tiliaceus* leaf extract were analyzed using FTIR to know the phytochemical compounds responsible for the synthesized ZnO NPs. The appearance of peaks at 3459 cm^{-1} ascribed to OH stretching vibration of O–H groups in water, alcohol, and phenol. The wavenumber at 2069 cm^{-1} is due to the asymmetric stretching of C–H groups. The intense band at 1534 cm^{-1} relates to the C=C stretch in the aromatic ring, and C=O stretch in polyphenols compounds[25]. The band at 1415 cm^{-1} is due to the presence of tertiary alcohol (C-OH). Stretching vibrations located

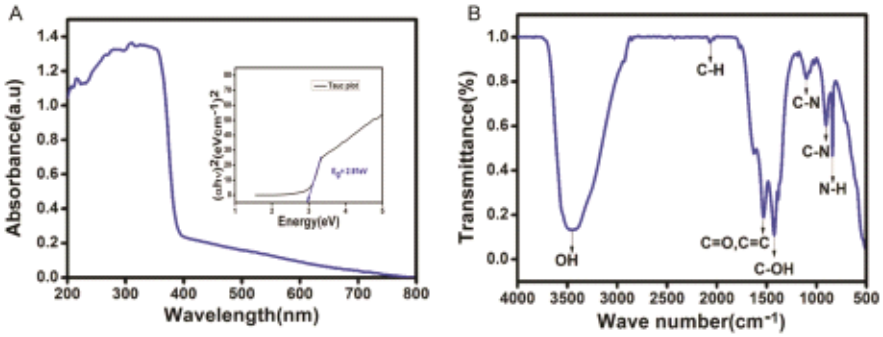

Fig. 2 — (A) UV-Vis spectroscopy of ZnO NPs; and (B) FTIR spectroscopy of ZnO NPs

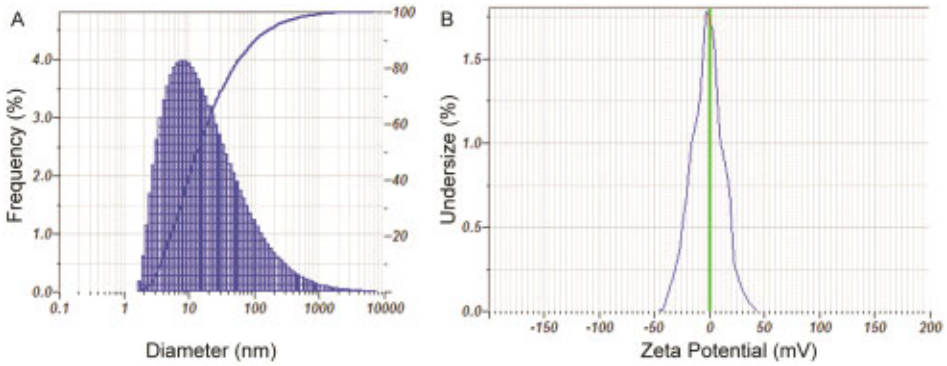

Fig. 3 — (A) DLS pattern of ZnO NPs; and (B) Zeta potential of ZnO NPs

at 905 and 841 cm^{-1} represented C−N stretching and N−H was of amines, respectively. Thus, from the FTIR spectrum concluded that phenolics and flavonoids of *H. tiliaceus* leave extract have been involved in the synthesis of ZnO NPs through reduction and stabilization action[14,15].

Particle size analysis (PSA) and zeta potential study

Dynamic light scattering (DLS) was performed to determine the particle size distribution and average particle size of ZnO NPs. The average particle size of ZnO NPs was 30 to 60 nm (Fig. 3A). The size of ZnO NPs was further evaluated by TEM. The average zeta potential value of ZnO NPs was − 1.2 mV (Fig. 3B). The negative charge of ZnO NPs could be due to the acidic phytochemicals of *H. tiliaceus* and thus, provides the stability at a persistent long period of time.

XRD analysis

The *H. tiliaceus* mediated synthesized ZnO NPs crystal lattice structure was carried out by X-ray diffraction analysis (Fig. 4A). The XRD analysis angle range was predetermined to be from 10°-90°. The spectrum obtained indicated the hexagonal phase structure with specific reflections at 32.05°, 34.92°, 36.51°, 47.51°, 57.10°, 63.14°, 66.60°, 68.18° and 69.34° corresponding to (100), (002), (101), (102), (110), (103), (200), (112), and (201) orientations, respectively, which are in confirmation with the JCPDS data card no-89-1397. As per the data obtained from XRD, the mean crystalline size (D) of the ZnO NPs was calculated using Debye Scherrer's formula:

$$D = K\lambda/\beta\cos\theta$$

where, 'λ' is the wavelength of the X-ray radiation employed and equal to 1.5406. The symbol 'θ' is full width at half its maximum intensity of diffraction pattern (FWHM) in radian is the Bragg diffraction angle. In our study, average crystal size was determined as 16 nm from Debye Scherrer's formula. The obtained result of the present XRD study was inconsistent with previous reports[26,27]. The XRD study concluded that the lattice structure of as-synthesized ZnO NPs was crystalline in nature.

HR-TEM and SAED analysis

A high-resolution transmission electron microscope (HR-TEM) was used to examine the size, shape, and morphology of as-synthesized ZnO NPs. Figure 4B shows a HR-TEM image of *H. tiliaceus* mediated synthesized ZnO NPs and a selective area electron diffraction (SAED) pattern. The size of ZnO NPs ranges from 30 to 60 nm and they are spherical in

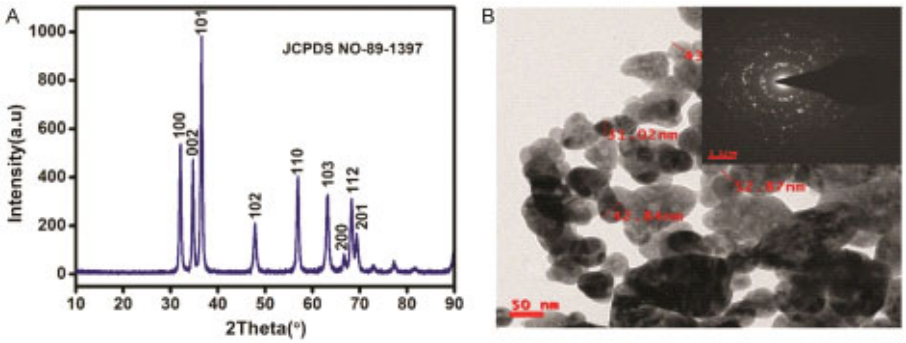

Fig. 4 — (A) XRD pattern of ZnO NPs; and (B) HR-TEM image and SAED pattern of ZnO NPs

Table 1 — Antibacterial activity of ZnO NPs against pathogenic bacterial strains by the zone of inhibition assay

S. No	Bacterial strain	Zone of inhibition (mM)			
		Concentration of ZnO NPs			
		25 µg	50 µg	75 µg	100 µg
1	*Bacillus subtilis* (MTCC - 441)	10 mM	11 mM	12 mM	14 mM
2	*Staphylococcus aureus* (MTCC - 1430)	8 mM	9 mM	11 mM	12 mM
3	*Klebsiella pneumoniae* (MTCC - 7162)	10 mM	12 mM	13 mM	16 mM
4	*Pseudomonas aeruginosa* (MTCC - 4996)	10 mM	12 mM	14 mM	15 mM
5	*Proteus vulgaris* (MTCC-744)	6 mM	6 mM	8 mM	10 mM
6	*Escherichia coli* (MTCC - 443)	10 mM	11 mM	12 mM	14 mM

shape. The SAED pattern provided information that ZnO NPs have crystallinity and have an index with an interplanar distance of 2.94.

Antibacterial activity of ZnO NPs

H. tiliaceus mediated synthesized ZnO NPs showed potential antibacterial activity against six bacterial strains, two Gram-positive: *B. subtilis* (MTCC - 441) and *S. aureus* (MTCC - 1430), and four Gram-negative: *K. pneumoniae* (MTCC - 7162), *P. aeruginosa* (MTCC - 4996), *P. vulgaris* (MTCC - 744), and *E. coli* (MTCC no: 443). The maximum zone of inhibition of the ZnO NPs against *K. pneumoniae* and *P. aeruginosa* (Table 1). This can be accredited to the generation of zinc oxide ions from ZnO NPs. The results obtained were in agreement with the existing literature. The green synthesized ZnO NPs from the extract of *H. tiliaceus* leaf reported potent antimicrobial activities.

According to Lakshmeesha *et al.*, the accumulation of reactive oxygen species (ROS) generated by nanoparticles (NPs) is the fundamental explanation for antibacterial action[14]. According to Zhang *et al.* nanoparticles (NPs) have antibacterial activity due to a chemical interaction between membrane proteins and hydrogen peroxide, or other chemical agents generated in the presence of nanoparticles (NPs) by the bacteria cell's lipid bilayer[29]. Padmavathy & Vijayaraghavan studied further into detail about nanoparticles antibacterial activity (NPs) and reported that nanoparticles produced by the precipitation reaction of zinc acetate hydrolysis in 2-propanol showed a unique bacterial growth inhibitory activity against *E. coli*. According to reports, the ROS molecules generated by ZnO NPs penetrate the bacteria's cell membrane and induce death[30].

Anticancer activity of ZnO NPs

The anticancer activity of ZnO NPs was studied against human breast cancer cell lines MCF-7 at varying concentrations and results have been illustrated in (Fig. 5). It is evident from the graph that an initial concentration of as low as 20 µg/mL had triggered anticancer action against the MCF-7 cell lines. The cell viability of MCF-7 cells was reduced with a dose of ZnO NPs and exhibited a dose-dependent manner. The IC_{50} value was calculated to be 65.83 ± 2.57 µg/mL (Fig. 5A). The existence of synergy between NPs and the covering polyphenols of the leaf extract are responsible for elevated anticancer activity of the ZnO NPs. The cancer cells have a higher uptake of the ZnO NPs as against the normal healthy cells and this, in turn, is responsible for the greater cytotoxicity of ZnO NPs against cancerous cells. The cancerous cells have an irregular metabolism and high proliferation rate that makes them more vulnerable[31]. The coordinated increase in the production of ROS and also the constraints on the

transcription process are caused by the synchronized effect of ZnO NPs and polyphenols[32]. Notably, antioxidants such as polyphenols display cytotoxicity only against abnormal cells[2]. Cells experiencing toxicity have been noted by cellular rounding, contraction in the membrane, and loss of cell adhesion ability (Fig. 5B).

Dye degradation activity of ZnO NPs

The catalytic reduction performance of the as-synthesized ZnO NPs was evaluated on catalytic reduction of MB, MO, and MG dyes using $NaBH_4$ as a reducing agent. The reduction process was monitored by UV-vis spectrophotometer absorbance reading with λ_{max} at 664 nm, 464 nm, and 615 nm for MB, MO, and MG, respectively.

To study the efficacy of the ZnO NPs to degrade a dye the degradation process was carried out in two processes. In the first process, only $NaBH_4$ was reacted with the dyes and absorbance readings were noted. In the second process, dyes were reacted with $NaBH_4$ along with ZnO NPs and the spectrophotometer absorbance reading was taken. The absorbance peaks at λ_{max} for all three dyes showed a gradual decrease in the absorbance peaks confirming the dye degradation took place as well the fading of the color is also visible after the addition of ZnO NPs. As shown in Figure 6 the time taken for the ZnO NPs as a catalyst in the presence of $NaBH_4$ as a reducing agent are 16 min, 28 min, and 12 min for MB, MO, and MG, respectively.

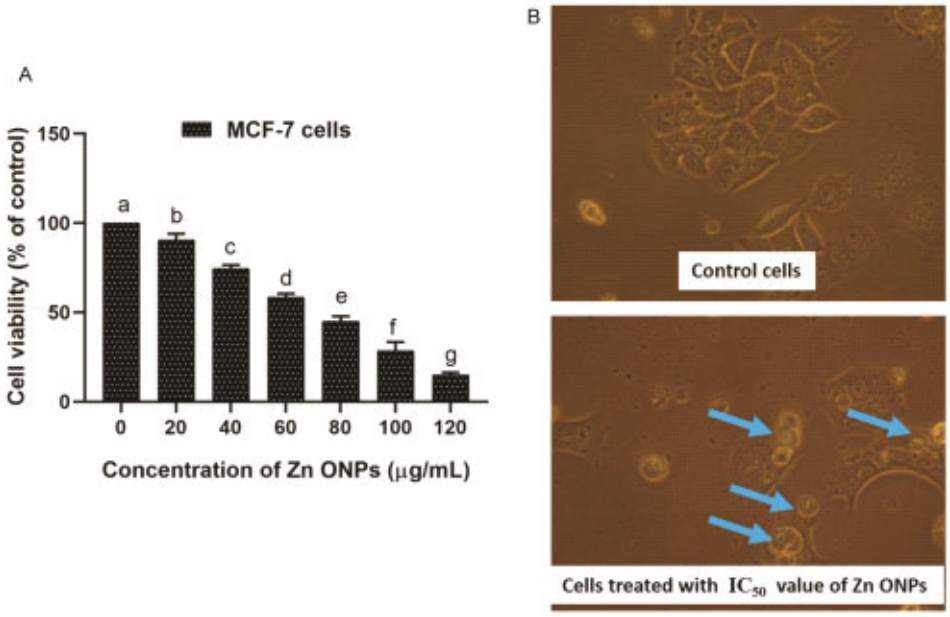

Fig. 5 — (A) Anticancer activity of ZnO NPs against MCF-7 cells determined by MTT assay. The experiments were executed in six replicates (n = 6). The results were represented as mean ± standard deviation. The data were analyzed by one-way ANOVA and statistical difference between test samples was analyzed by Tukey's test. The *P*-value ≤ 0.05 was considered significant. The bars with different alphabetic was significant (*P*-value ≤ 0.05); and (B) Microscopic images of control cells and cells treated with IC_{50} value of ZnO NPs (65.83 ± 2.57 µg/mL). The images were captured at 400x

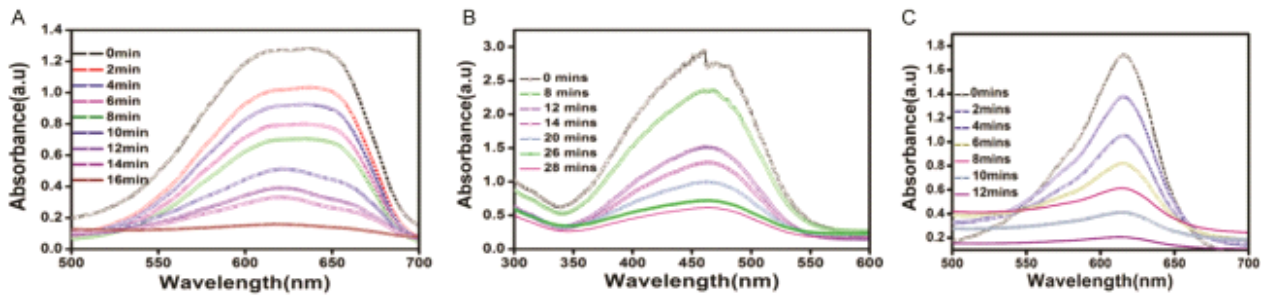

Fig. 6 — Dye degradation efficacy of ZnO NPs on (A) methylene blue; (B) methyl orange; and (C) malachite green dyes at a different wavelength

The percentage of dye degradation was calculated from the following equation:

$$\text{Dye degradation (\%)} = (C_0 - C)/C_0 \times 100$$

where, C_0 was the initial amount of dye and C was the left-over amount of dye after the degradation process. The study finds 95%, 85%, and 88% of the degradation for MB, MO, and MG degradation, respectively (Fig. 7).

The kinetics studies for all three reactions were spectrophotometrically monitored at absorption at λ_{max} for three dyes respectively. As the concentration of $NaBH_4$ is more than that of the dyes in all the reactions, its concentration remains constant during the entire reaction, and hence the reaction follows pseudo-first order kinetics. The rate equation adopted was as follows:

$$k = \ln[A_t]/[A_0]$$

where, k was the pseudo-first order rate constant, $[A_o]$ was the initial concentration of the dye, and $[A_t]$ was the concentration at '*t*' time.

Following, for the constant catalyst concentration, a graph with a plot of ln (A_t/A_o) with respect to time (min) shows the straight line of slope k in (Fig. 8). The rate constant (k) for degradation of MB, MO, and MG by $NaBH_4$ in presence of ZnO NPs was calculated to be 0.250 min^{-1}, 0.126 min^{-1}, and 0.326 min^{-1}, respectively. The regression value for MB, MO, and MG were 0.98364, 0.97899, and 0.99211, respectively. Thus, the kinetic values also prove that the dye degradation ability of ZnO NPs as a nanocatalyst in the presence of $NaBH_4$ as a reducing agent is reliable.

In support of our study, Rambabu *et al*. green synthesized ZnO NPs from *Phoenix dactylifera* waste

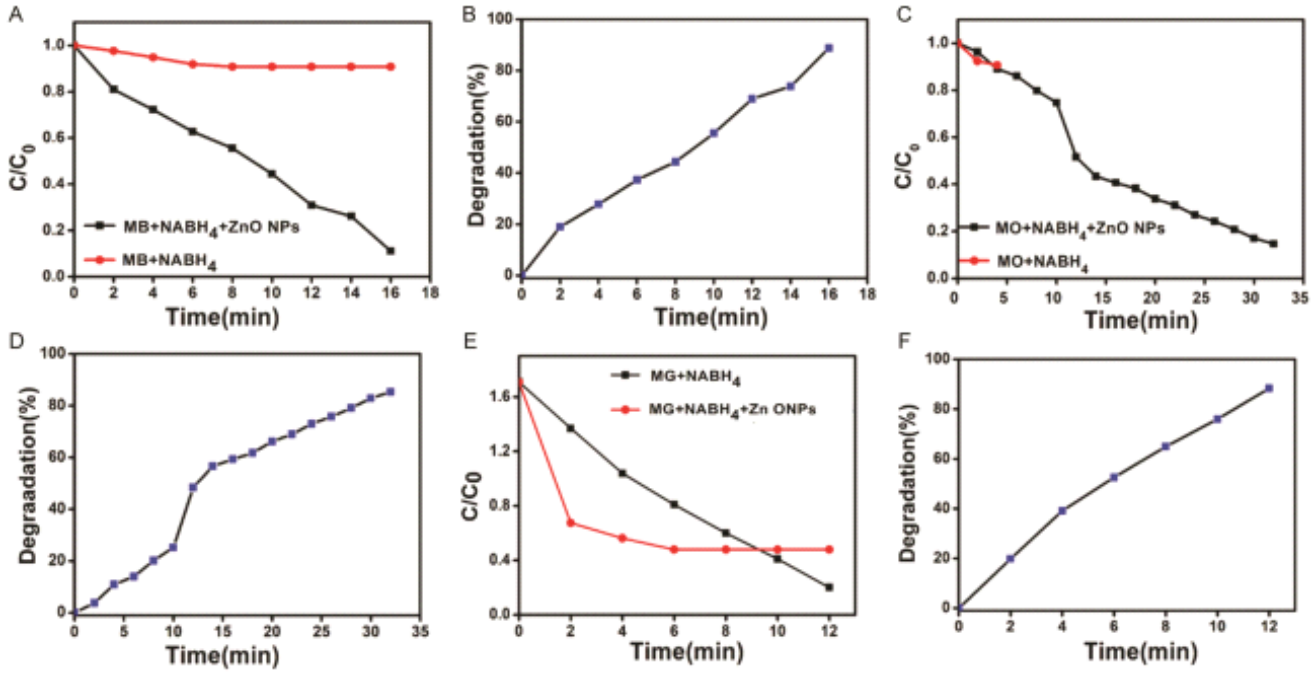

Fig. 7 — Dye degradation efficacy plots (C/C_0 Vs time) of ZnO NPs on (A) methylene blue; (C) methyl orange; and (E) malachite green dyes. Dye degradation percentile of ZnO NPs on (B) methylene blue, (D) methyl orange; and (F) malachite green dyes

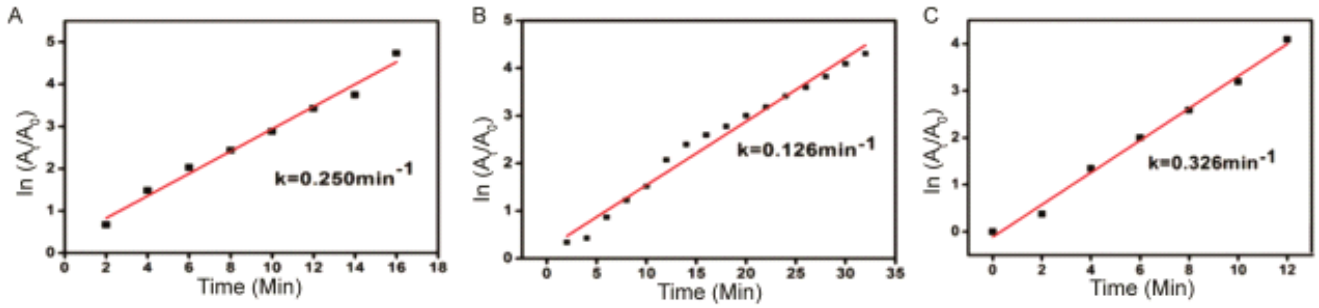

Fig. 8 — Kinetic graphs for dye degradation activity of ZnO NPs on (A) methylene blue; (B) methyl orange; and (C) malachite green dyes

and revealed 90% dye degradation capacity on hazardous MB dye and eosin yellow dyes[33]. Moghaddas *et al*. biosynthesized ZnO NPs using quince seed mucilage and demonstrated 80% degradation of MB dye within 2 h[34]. Similarly, Brindhadevi *et al*. ZnO NPs prepared from hybrid grape pulp extract and showed complete degradation of MG dye[35]. The present study and previous reports showed that ZnO NPs could be highly useful for the clean-up of hazardous dyes from the environment.

Conclusion

The focus of this research was to synthesize ZnO NPs from an aqueous leaf extract of *H. tiliaceus*. The synthesized ZnO NPs were found with an average size of 60 nm and a spherical form. The presence of phenols and flavonoids in the phytochemical analysis of *H. tiliaceus* revealed that they are the key contributors to reduction as well as capping agents for ZnO NPs synthesis. The as-synthesized ZnO NPs exhibited potent antibacterial activity against Gram-negative and Gram-positive bacteria by well diffusion technique. The as-synthesized ZnO NPs displayed potent anticancer activity against MCF-cells by cell viability technique MTT assay. The ZnO NPs were also tested for their ability to degrade methylene blue, methyl orange, and malachite green dyes, all of which are industrial waste, and the results showed that 95%, 85%, and 88% of the degradation, respectively. The percentage of degradation was discovered to be significantly affected by the concentration of ZnO NPs and the time of illumination. This research will shed light on new metal oxide catalysts and demonstrate the utility of ZnO NPs as a nanocatalyst for environmental clean-up.

Acknowledgement

Vinay Viswanath Konduri and Sudhakar Podha were thankful to Acharya Nagarjuna University for providing the facility. Also, Vinay Viswanath Konduri and Sudhakar Podha were thankful to Venkateswara Rao Kalagadda for providing nano science and technology facilities at Jawaharlal Nehru Technological University, Hyderabad. Naveen Kumar Kalagatur was thankful to DST-SERB for providing a National Post-Doctoral Fellowship (File no: PDF/2019/002483). Anusuya Nagaraj was thankful to DST-PURSE for providing fellowship.

Conflict of interest

All authors declare no conflict of interest.

References

1 Sundararaj N, Kalagatur NK, Mudili V, Krishna K & Antonysamy M, Isolation and identification of enterotoxigenic *Staphylococcus aureus* isolates from Indian food samples: Evaluation of in-house developed aptamer linked sandwich ELISA (ALISA) method. *J Food Sci Technol*, 56 (2019) 1016.

2 Chen AY & Chen YC, A review of the dietary flavonoid, kaempferol on human health and cancer chemoprevention. *Food Chem*, 138 (2013) 2099.

3 Elango G, Roopan SM. Efficacy of SnO_2 nanoparticles toward photocatalytic degradation of methylene blue dye. *J Photochem Photobiol B: Biol*, 155 (2016) 34.

4 Chen Z, Li XX, Du G, Chen N & Suen AY, A sol–gel method for preparing ZnO quantum dots with strong blue emission. *J Lumin*, 131(2011) 2072

5 Lu JG, Ye ZZ, Huang JY, Zhu LP, Zhao BH, Wang ZL & Fujita S, ZnO quantum dots synthesized by a vapor phase transport process. *Appl Phys Lett*, 88 (2006) 063110.

6 Seelig EW, Tang B, Yamilov A, Cao H & Chang RP, Self-assembled 3D photonic crystals from ZnO colloidal spheres. *Mater Chem Phys*, 80 (2003) 257.

7 Nagaraj A & Samiappan S, Presentation of antibacterial and therapeutic anti-inflammatory potentials to hydroxyapatite *via* biomimetic with *Azadirachta indica*: An *in vitro* anti-inflammatory assessment in contradiction of LPS-induced stress in RAW 264.7 Cells. *Front Microbiol*, 10 (2019) 1757.

8 Gunti L, Dass RS & Kalagatur NK, Phytofabrication of selenium nanoparticles from *Emblica officinalis* fruit extract and exploring its biopotential applications: antioxidant, antimicrobial, and biocompatibility. *Front Microbiol*, 10 (2019) 931.

9 Akhtar MS, Ameen S, Ansari SA & Yang O, Synthesis and characterization of ZnO nanorods and balls nanomaterials for dye sensitized solar cells. *J Nanoeng Nanomanuf*, 1 (2011) 71.

10 Bozetine H, Wang Q, Barras A, Li M, Hadjersi T, Szunerits S & Boukherroub R, Green chemistry approach for the synthesis of ZnO–carbon dots nanocomposites with good photocatalytic properties under visible light. *J Colloid Interface Sci*, 465 (2016) 286.

11 Wahab R, Kim YS, Lee DS, Seo JM & Shin HS, Controlled synthesis of zinc oxide nanoneedles and their transformation to microflowers. *Sci Adv Mat*, 2 (2010) 35.

12 Ashtaputre SS, Deshpande A, Marathe S, Wankhede ME, Chimanpure J, Pasricha R, Urban J, Haram SK, Gosavi SW & Kulkarni SK, Synthesis and analysis of ZnO and CdSe nanoparticles. *Pramana*, 65 (2005) 615.

13 Kajbafvala A, Ghorbani H, Paravar A, Samberg JP, Kajbafvala E & Sadrnezhaad SK, Effects of morphology on photocatalytic performance of Zinc oxide nanostructures synthesized by rapid microwave irradiation methods. *Superlattices Microstruct*, 51 (2012) 512.

14 Lakshmeesha TR, Kalagatur NK, Mudili V, Mohan CD, Rangappa S, Prasad BD, Ashwini BS, Hashem A, Alqarawi AA, Malik JA & Abd_Allah EF,. Biofabrication of zinc oxide nanoparticles with *Syzygium aromaticum* flower buds extract and finding its novel application in controlling the growth and mycotoxins of *Fusarium graminearum*. *Front Microbiol*, 10 (2019) 1244.

15 Rajan M, Anthuvan AJ, Muniyandi K, Kalagatur NK, Shanmugam S, Sathyanarayanan S, Chinnuswamy V, Thangaraj P & Narain N, Comparative study of biological (*Phoenix loureiroi* fruit) and chemical synthesis of chitosan-encapsulated zinc oxide nanoparticles and their biological properties. *Arab J Sci Eng*, 45 (2020) 15.
16 Lakshmeesha TR, Murali M, Ansari MA, Udayashankar AC, Alzohairy MA, Almatroudi A, Alomary MN, Asiri SM, Ashwini BS, Kalagatur NK & Nayak CS, Biofabrication of zinc oxide nanoparticles from *Melia azedarach* and its potential in controlling soybean seed-borne phytopathogenic fungi. *Saudi J Biol Sci*, 27 (2020) 1923.
17 Javanmardi J, Stushnoff C, Locke E & Vivanco JM, Antioxidant activity and total phenolic content of Iranian *Ocimum* accessions. *Food Chem*, 83 (2003) 547.
18 Yu J, Wang L, Walzem RL, Miller EG, Pike LM & Patil BS, Antioxidant activity of citrus limonoids, flavonoids, and coumarins. *J Agric Food Chem*, 53 (2005) 2009.
19 Singh RP, Shukla VK, Yadav RS, Sharma PK, Singh PK & Pandey AC, Biological approach of zinc oxide nanoparticles formation and its characterization. *Adv Mater Lett*, 2 (2011) 313.
20 Swaminathan S, Haribabu J, Kalagatur NK, Konakanchi R, Balakrishnan N, Bhuvanesh N & Karvembu R, Synthesis and anticancer activity of [RuCl2 (η6-arene)(aroylthiourea)] complexes—high activity against the human neuroblastoma (IMR-32) cancer cell line. *ACS Omega*, 4 (2019) 6245.
21 Swaminathan S, Haribabu J, Kalagatur NK, Nikhil M, Balakrishnan N, Bhuvanesh NS, Kadirvelu K, Kolandaivel P & Karvembu R, Tunable Anticancer Activity of Furoylthiourea-Based RuII–Arene Complexes and Their Mechanism of Action. *Chem Eur J*, 27 (2021):7418-33.
22 Wong SK, Lim YY & Chan EW, Antioxidant properties of Hibiscus: Species variation, altitudinal change, coastal influence and floral colour change. *J Trop For Sci*, 21 (2009) 307.
23 Wahab R, Ansari SG, Kim YS, Song M & Shin HS, The role of pH variation on the growth of zinc oxide nanostructures. *Appl Surf Sci*, 255 (2009) 4891.
24 Zhang C, Shao M, Ning F, Xu S, Li Z, Wei M, Evans DG & Duan X, Au nanoparticles sensitized ZnO nanorod@ nanoplatelet core–shell arrays for enhanced photoelectrochemical water splitting. *Nano Energy*, 12 (2015) 231.
25 Anbuvannan M, Ramesh M, Viruthagiri G, Shanmugam N & Kannadasan N, *Anisochilus carnosus* leaf extract mediated synthesis of zinc oxide nanoparticles for antibacterial and photocatalytic activities. *Mater Sci Semicond Process*, 39 (2015) 621.
26 Bhatia S & Verma N, Photocatalytic activity of ZnO nanoparticles with optimization of defects. *Mater Res Bull*, 95 (2017) 468.
27 Ramesh M, Anbuvannan M & Viruthagiri GJ, Green synthesis of ZnO nanoparticles using *Solanum nigrum* leaf extract and their antibacterial activity. *Spectrochim Acta A Mol Biomol Spectrosc*, 136 (2015) 864.
28 Yu Z, Li Q, Wang J, Yu Y, Wang Y, Zhou Q & Li P, Reactive oxygen species-related nanoparticle toxicity in the biomedical field. *Nanoscale Res Lett*, 15 (2020) 1.
29 Zhang L, Ding Y, Povey M & York D, ZnO nanofluids–A potential antibacterial agent. *Prog Nat Sci*, 18 (2008) 939.
30 Padmavathy N & Vijayaraghavan R, Enhanced bioactivity of ZnO nanoparticles—an antimicrobial study. *Sci Technol Adv Mater*, 9 (2008) 035004.
31 Muñoz-Pinedo C, El Mjiyad N & Ricci JE, Cancer metabolism: current perspectives and future directions. *Cell Death Dis*, 3 (2012) e248.
32 Jayarambabu N, Rao TV, Kumar RR, Akshaykranth A, Shanker K & Suresh V, Anti-hyperglycemic, pathogenic and anticancer activities of *Bambusa arundinacea* mediated Zinc Oxide nanoparticles. *Mater Today Commun*, 26 (2021) 101688.
33 Rambabu K, Bharath G, Banat F, Show PL. Green synthesis of zinc oxide nanoparticles using *Phoenix dactylifera* waste as bioreductant for effective dye degradation and antibacterial performance in wastewater treatment. *J Hazard Mater*, 402 (2021) 123560.
34 Moghaddas SM, Elahi B & Javanbakht V, Biosynthesis of pure zinc oxide nanoparticles using Quince seed mucilage for photocatalytic dye degradation. *J Alloys Compd*, 821 (2020) 153519.
35 Brindhadevi K, Samuel MS, Verma TN, Vasantharaj S, Sathiyavimal S, Saravanan M, Pugazhendhi A & Duc PA, Zinc oxide nanoparticles (ZnONPs)-induced antioxidants and photocatalytic degradation activity from hybrid grape pulp extract (HGPE). *Biocatal Agric Biotechnol*, 28 (2020) 101730.